ISTITUTO NAZIONALE DI FISICA NUCLEARE

Sezione di Catania

INFN/BE-77/2
13 Luglio 1977

N. Arena, M. Lattuada, F. Riggi, C. Spitaleri and D. Vinciguerra:

ENERGY DEPENDENCE OF THE QUASI-FREE $^{9}Be(^{3}He,\alpha\alpha)^{4}He$ REACTION NEAR THE COULOMB BARRIER.

Servizio Documentazione
dei Laboratori Nazionali di Frascati

Istituto Nazionale di Fisica Nucleare
Sezione di Catania

INFN/BE-77/2
13 Luglio 1977

N. Arena, M. Lattuada(x), F. Riggi(x), C. Spitaleri(o) and D. Vinciguerra: ENERGY DEPENDENCE OF THE QUASI-FREE $^{9}Be(^{3}He, \alpha\alpha)\,^{4}He$ REACTION NEAR THE COULOMB BARRIER(+).

ABSTRACT:

The coincidence detection of two α-particles emitted in the $^{9}Be(^{3}He,\alpha\alpha)\,^{4}He$ reaction shows evidence for quasi-free processes even for low incident energies. At 2.5 and 2.7 MeV the impulse distribution of the α-cluster in ^{9}Be can be deduced in PWIA. The excitation function has been obtained at $\theta_{CM}=90^{o}$ together with that of the sequential reaction proceeding through the 16.6 and 16.9 MeV levels of ^{9}Be. The behaviour of the excitation functions for energies around the Coulomb barrier is also discussed.

1. - INTRODUCTION

While there has been in the past considerable interest in the study of quasi-free scattering (QFS) and valuable informations on the wave function of nucleons and clusters have been obtained, quasi-free reactions (QFR) have been used only recently as an important tool of investigation of the structure of light nuclei and of the reaction mechanism for those processes involving more than two particles in the final state[1, 2].

The analysis of QFS or QFR experiments is usually done in the plane wave (PWIA) or distorted wave (DWIA) impulse approximation since it is greatly simplified by the factorization of the cross section. Though it is well known that the interpretation of QF data is influenced by the presence of multiple scattering, off-energy shell effects or absorption, PWIA is generally used for its simplicity. On the other hand PWIA predicts reasonably well the shape of the experimental momentum distribution, at least for high incident energies and small values of the nucleon or cluster moment[3], but it yields cross sections larger than the experimental ones, so that a coefficient $P < 1$ (that takes into account clustering probability and absorption effects) has to be introduced in the theoretical predictions.

With these assumptions, PWIA gives, for the coincidence cross section of the reaction N(0, 1. 2)S, where N=S+T (Fig. 1), the following expression:

$$\frac{d^{3}\sigma}{d\Omega_{1}\, d\Omega_{2}\, dE_{1}} = P\,(KF)\,\left(\frac{d\sigma}{d\Omega}\right)_{OT}\, G^{2}\,(p_{S}) \qquad (1)$$

(x) Centro Siciliano di Fisica Nucleare e di Struttura della Materia, Catania
(o) Istituto di Meccanica Razionale e Matematiche Applicate all'Ingegneria dell'Università di Catania.
(+) Work supported in part by Istituto Nazionale di Fisica Nucleare, Sezione di Catania, and by Centro Siciliano di Fisica Nucleare e di Struttura della Materia, Catania.

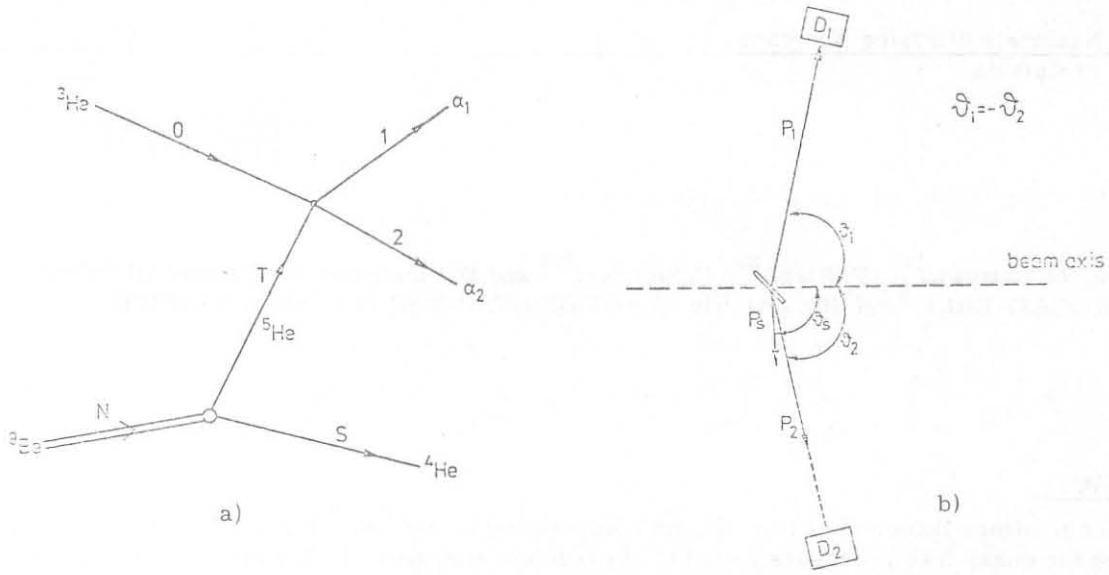

FIG. 1 - a) Interpretation of the (^{3}He, $\alpha\alpha$) reaction in ^{9}Be in terms of quasi-free reaction. b) The two detectors D_1 and D_2 allow the determination of $\vec{p}_1$ and $\vec{p}_2$, so that the momentum $\vec{p}_S$ of the spectator cluster can be deduced.

where (KF) is a kinematical factor given by

$$(KF) = \frac{k_1 k_2}{\hbar^2 k_o} m_2 \left(\frac{m_o + m_2}{m_2}\right)^2 \left[1 + \frac{m_2}{m_S} + \frac{m_2 k_1}{m_S k_2} \cos\theta_{12} - \frac{m_2 k_o}{m_S k_2} \cos\theta_2\right]^{-1} \qquad (2)$$

where m_i and k_i are the masses and wave numbers of the incident particle 0, of the two detected particles 1 and 2 and of the spectator S (Fig. 1), while θ_{12} is the angle between particles 1 and 2, $(d\sigma/d\Omega)_{OT}$ is the cross section for the off-energy-shell

$$^5\text{He}\ (^3\text{He}, \alpha)\ ^4\text{He} \qquad (3)$$

reaction, and

$$G(\vec{p}_S) = \int \chi(\vec{r}) \exp(-i \vec{p}_S \vec{r})\, d\vec{r}, \qquad (4)$$

the Fourier transform of the intercluster wave function $\chi(\vec{r})$, is the momentum distribution of the spectator cluster S.

It is generally assumed that the condition for QFS or QFR is that the involved momenta be at least of the order of 300 MeV/c, with an associated wavelenght of about 0.7 fm. This value corresponds to 50, 25 and 13 MeV for protons, deuterons and α-particle respectively. Nevertheless, QFS has already been studied at lower energies. For instance, the ^{6}Li(d, dd) ^{4}He QFS has been studied (see ref. (4)) for energies ranging between 6 and 11 MeV.

In the case of the ^{9}Be(^{3}He,$\alpha\alpha$) ^{4}He reaction, which has a high Q value (19.09 MeV), the high momentum condition is satisfied only by the outgoing α-particles for energies lower than, say, 13 MeV. The experiment has however shown evidence[1, 2] for the existence of QF effects at incident energies as low as 4 and 2.8 MeV. The results have been interpreted in PWIA and the ^{9}Be nucleus has been considered as made up by ^{4}He and ^{5}He clusters, according to evidence obtained also with QFS at high energy[3, 5].

The aim of the present work was the study of the same reaction at energies lower than 2.8 MeV in order to:

a) follow the behaviour of the momentum distribution $G^2(p_S)$ to very low energies;

b) study the excitation function of the QF process around the Coulomb barrier.

We have then performed measurements for several ^{3}He energies between 1.0 and 2.7 MeV, by detecting two α-particles in coincidence (Fig. 1b) and recording a bidimensional E_1-E_2 spectrum, where E_1 and E_2 are the α-particle kinetic energies. QFR was expected to contribute with a broad distribution in the kinematical locus of the E_1-E_2 spectrum, while peaks would indicate sequential processes

$$^3\mathrm{He} + {}^9\mathrm{Be} \longrightarrow {}^8\mathrm{Be}^* + \alpha \qquad {}^8\mathrm{Be}^* \rightarrow \alpha + \alpha \tag{5}$$

proceeding through the ground state or the excited levels of ^{8}Be. The measurements were performed in the energy sharing mode since, as we have already shown, it introduces less distortions and unknown factors with respect to the angular correlation mode. Data taking is also faster.

2. - THE EXPERIMENT.

The experiment was carried out at the Van de Graaff accelerator of the CSFN-SM laboratories in Catania. A 190 μg/cm^2 ^{9}Be target, evaporated on a 40 μg/cm^2 ^{12}C backing, was used to make absolute measurements of $d^3\sigma / d\Omega_1 d\Omega_2 dE_1$ for several incident energies from 1.0 to 2.7 MeV. The ^{3}He beam was captured in a Faraday cup and the beam current was integrated using a standard current indicator-integrator. The beam current was usually around 200 nA.

For each run two outgoing particles were detected by ORTEC silicon surface-barrier detectors placed at the symmetrical angles $\theta_1 = -\theta_2$ (in coplanar geometry) chosen in such a way that it was possible to accept the condition $\vec{p}_S = 0$ when $p_1 = p_2$ and $m_1 = m_2$. This condition gives

$$\cos^2 \theta_1 = \frac{m_o}{m_1} \quad \frac{E_o}{E_o + Q}$$

The solid angle of each detector was 3 msr. The absolute normalization of the ^{9}Be (^{3}He, $\alpha\alpha$) ^{4}He reaction cross section was obtained by monitoring in a third detector the ^{3}He ions elastically scattered from the ^{9}Be target and the ^{12}C backing.

Checks were made to determine whether the beam direction coincided with the axis of the scattering chamber by comparing the yield of elastically scattered ^{3}He measured by the two detectors placed at equal angles on the sides of the beam axis.

Energy pulses from the detectors were sent to a LABEN 4096 channel pulse-height analyser operating in a 64x64 two-dimensional mode and gated by a COSMIC fast-slow coincidence.

As in the previous experiment[2] the target was set at 45° with respect to the beam direction. In this way the energy E_1 of the α-particle measured from detector 1 is reduced by an amount practically independent of the depth in which the reaction takes place.

3. - DATA ANALYSIS.

3.1. - Energy Spectra.

A bidimensional energy spectrum is shown in Fig. 2, for an incident energy $E_o = 2.7$ MeV. Coincident events are seen to fall mainly on the kinematical locus of the ^{9}Be(^{3}He, $\alpha\alpha$) ^{4}He reaction. Two different accumulation regions can be distinguished. The label A marks the region where a broad distribution is centered around the point $p_S = 0$ (marked by an arrow). Peaks corresponding to sequential processes (5) are indicated by label B. In Fig. 3 some of the measured α-α coincidence spectra are shown, for four different values of the incident energy. These and the other spectra, at even lower energy, were obtained by projecting on the E_1 axis the bidimensional coincidence spectrum. In the upper part of the figures are also reported the relative energies E_{12}, E_{1S}, and E_{2S}

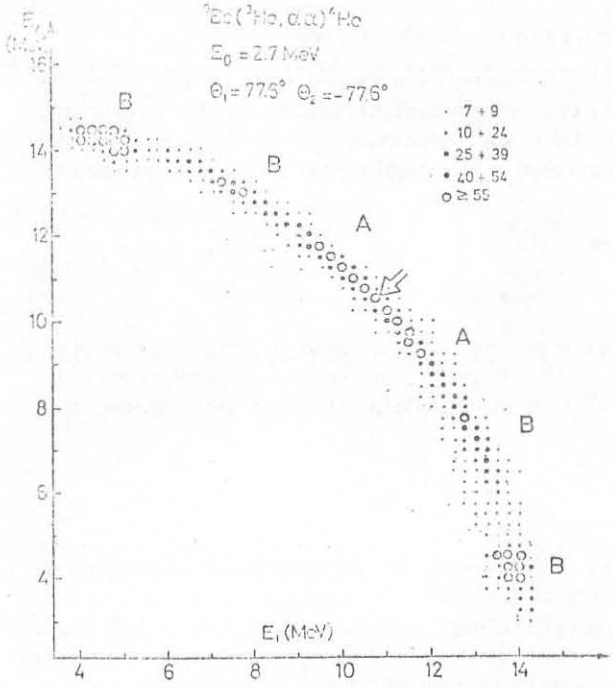

FIG. 2- Example of two dimensional energy spectrum. Regions B are peaks due to sequential processes, while in the broad region A only QF events are present. The arrow marks the point where $\vec{p}_S = 0$.

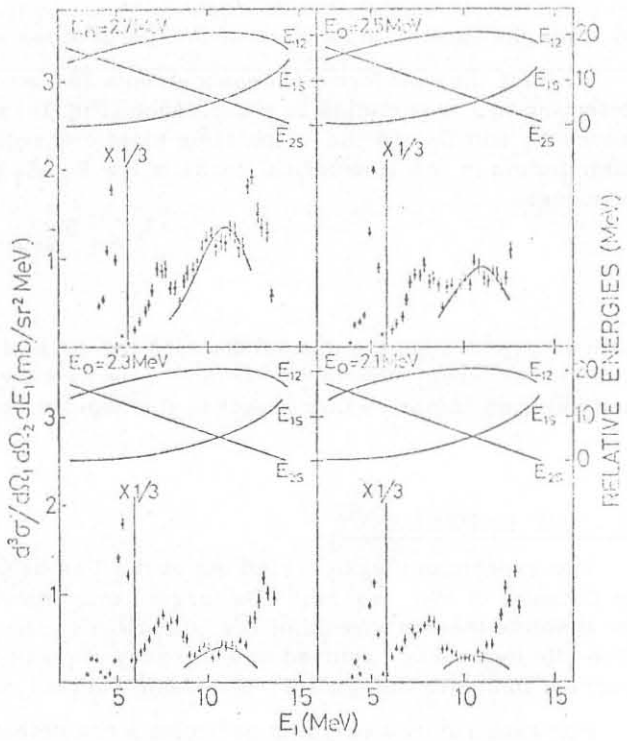

FIG. 3- α - α coincidence spectra projected on the E_1 axis, for various values of the incident energy. Only statistical errors are reported. The curves in the upper part of the spectra represent the relative energies E_{1S}, E_{2S} and E_{12}.

for any couple of α-particles in the final state.

This allows the identification of the peaks B appearing in the spectra. In fact, the sequential processes (5) proceeding through the excited levels of ^{8}Be, can be seen to contribute largely to the reaction. For instance, the peak around E_1=5 MeV (Fig. 3) is due to coincidence detection of the two α--particles coming from the decay of the 16.6 -16.9 MeV doublet. The state is easily identified from the value of the relative energy E_{12} at the peak position.

3. 2. - Momentum Distribution.

For each bombarding energy the detection angles were kept fixed (Sect. 2) and the energy sharing method was used to determine the impulse distribution. It has already been pointed out[2] that this method should introduce less distortions in the impulse distribution than the angular correlation. In fact, besides the relative energy E_{12} between the two detected α-particles, also the relative energy E_{OT} between the incident particle and the moving cluster, varies very slowly in the p_S region we are interested in. This allows us to consider $(d\sigma/d\Omega)_{OT}$ as a constant to extract $G^2(p_S)$.

Since the product $P \cdot (d\sigma/d\Omega)_{OT}$ of eq. (1) is then an unknown constant, the $G^2(p_S)$ distributions have been obtained in relative units only. Fig. 4 reports the momentum distributions obtained for E_o=2.7 and 2.5 MeV. The error bars include only the statistical errors.

We have performed fits of the experimental momentum distribution by assuming an intercluster wave function

$$\chi(\vec{r}) = R(r) \cdot Y_{oo}(\theta, \phi)$$

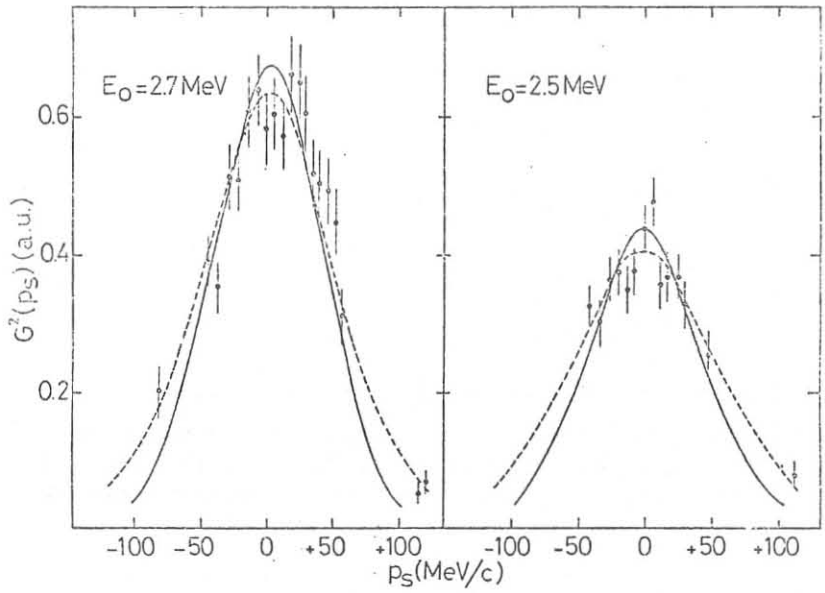

FIG. 4- Momentum distributions obtained from the α - α coincidence spectra at E_o=2.5 and 2.7 MeV. The dashed curves are fits obtained through Fourier transform of Eckart wave function (see text). If b is put equal to 0.35 fm^{-1} (Table I) the continuous curve fit is obtained

TABLE I - Values of the parameters for the various fits of $G^2(p_S)$. The functions refer to the radial part of the intercluster wave function. The fixed value b=0.35 fm^{-1} gives a correct size of the root mean square radius of ^{9}Be.

TYPE of FUNCTION	E_o (MeV)	R_c (fm)	b (fm^{-1})	χ^2	FWHM (MeV/c)
HÄNKEL	2.5	0.53	----	1.29	129
	2.7	1.48	----	1.50	116
	2.8[a]	1.20	----	1.40	115
ECKART	2.5	----	2.65	1.33	127
	2.7	----	0.90	1.34	115
	2.8[a]	----	1.67	1.40	118
ECKART (b fixed)	2.5	----	0.35	2.44	97
	2.7	----	0.35	1.96	97
	2.8[a]	----	0.35	2.10	97

a) ref. (2).

for s-wave only. Actually an α - cluster can be in a relative s or d state in ^{9}Be but the possible presence of the d-wave cannot be seen in our experiment since it would give a very small contribution to the impulse distribution for large p_S values[3].

For the radial part R(r) we used two different functions:

a) Hankel function with cut-off

$$R(r) = \begin{cases} 0 & r < R_c \\ (2k)^{1/2} \dfrac{\exp(-kr)}{r} & r > R_c \end{cases}$$

with $k=(2\mu B)^{1/2}$, μ being the reduced mass of ^{4}He-^{5}He system and B=2.52 MeV the α-particle binding energy in ^{9}Be.

b) Eckart functions. The Eckart function of order n is given by:

$$R_n(r)=N_n \left[1 - \exp(-br)\right]^{n+1} \frac{\exp(-kr)}{r}$$

with

$$N_n^{-2} = \sum_{l=0}^{2n+2} \binom{2n+2}{l} \frac{(-1)^l}{(lb+2k)}$$

and

$$G_n(p) = \sqrt{4\pi}\, N_n \sum_{l=0}^{n+1} \binom{n+1}{l} \frac{(-1)^l}{(lb+k)^2 + p^2}$$

The best fit values of the parameters of functions a) and b) with n=1 are listed in Table I.

The Fourier transform of the Hankel function gives fits very near to those obtained using the Eckart function, with the same numbers of adjustable parameters. If we fix b=0.35 fm^{-1} we obtain a correct value of the root mean square radius $\sqrt{\langle R_{Be}^2 \rangle}$ of ^{9}Be, where from classical considerations[2]

$$\sqrt{\langle R_{Be}^2 \rangle} = 1/2 \left[2(\langle r_4^2 \rangle + 25/81 \langle r^2 \rangle) + 2(\langle r_5^2 \rangle + 16/81 \langle r^2 \rangle)\right]^{1/2}$$

Using the relationship

$$\langle r^2 \rangle = N^{-2} \sum_{l=0}^{4} \binom{4}{l} \frac{(-1)^l}{(lb+2k)^3}$$

valid for function b) and the values $\sqrt{\langle r_4^2 \rangle}$ = 1.67 fm and $\sqrt{\langle r_5^2 \rangle}$ = 1.95 fm for the radii of the ^{4}He and ^{5}He clusters respectively, we obtain $\sqrt{\langle R_{Be}^2 \rangle}$ = 2.52 fm.

With the above value of b, we have still a good fit with a smaller width, FWHM =97 MeV/c.

The dashed curves in Fig. 4 refers to the fit obtained with the Hankel and Eckart functions, whilst the continuous one represents the fit obtained by fixing the value of b in the Eckart function.

Due to the finite angular resolution of the detectors we estimated that the actual widths of the momentum have been increased by about 5 MeV/c, so that the reported experimental values of the FWHM have been corrected accordingly. As it has already been pointed out[2] these values of the FWHM are in good agreement with the findings of experiments performed at higher energy and momentum transfer and with the results of the ^{9}Be(e, e' α) experiment[5].

A more correct treatment of the intercluster wave function should take into account the fact that it is a 3s-state[3]. Nevertheless the use of the function a) is widespread for its simplicity, while function b) allows to take in due account the finite extension of ^{9}Be. Moreover since in eq. (4) the r^2 weighing factor emphasizes the contribution to the integral of the asymptotic part of R(r), $G(p_S)$ depends weakly on the detailed shape of R(r) for small values of r. For the same reason, antisymmetrization can be neglected. We did not find it useful to try a more sophisticated form of R(r) for these facts and for the similarity of the fits already obtained.

4. - EXCITATION FUNCTIONS

To study the energy dependence of the quasi-free process in the ^{9}Be(^{3}He, $\alpha\alpha$) ^{4}He reaction near the coulombian barrier we have obtained its excitation function and compared it with that of the cross section for the sequential process (5) leaving the residual nucleus ^{8}Be in the excited levels at 16.6 and 16.9 MeV (not resolved).

The following procedure was adopted: first we assumed that the shape of $G^2(p_S)$ which fits the results at 2.7 and 2.5 MeV also holds for lower energies. Eq. (1) was then used to fit the experi-

mental results around $p_S=0$ by adjusting only its normalization factor. Examples of the fitting curves are reported in Fig. 3, where it is clear that the QFR contribution to the process can be overstimated for the lowest energies. The fits give a value for the product $P(d\sigma/d\Omega)_{QT}$ in eq. (1). Since P can reasonably be assumed to be a constant for the whole energy range, this procedure gives $(d\sigma/d\Omega)_{QT}$ for QF reaction (3) in arbitrary units. The results obtained are shown in Fig. 5a,

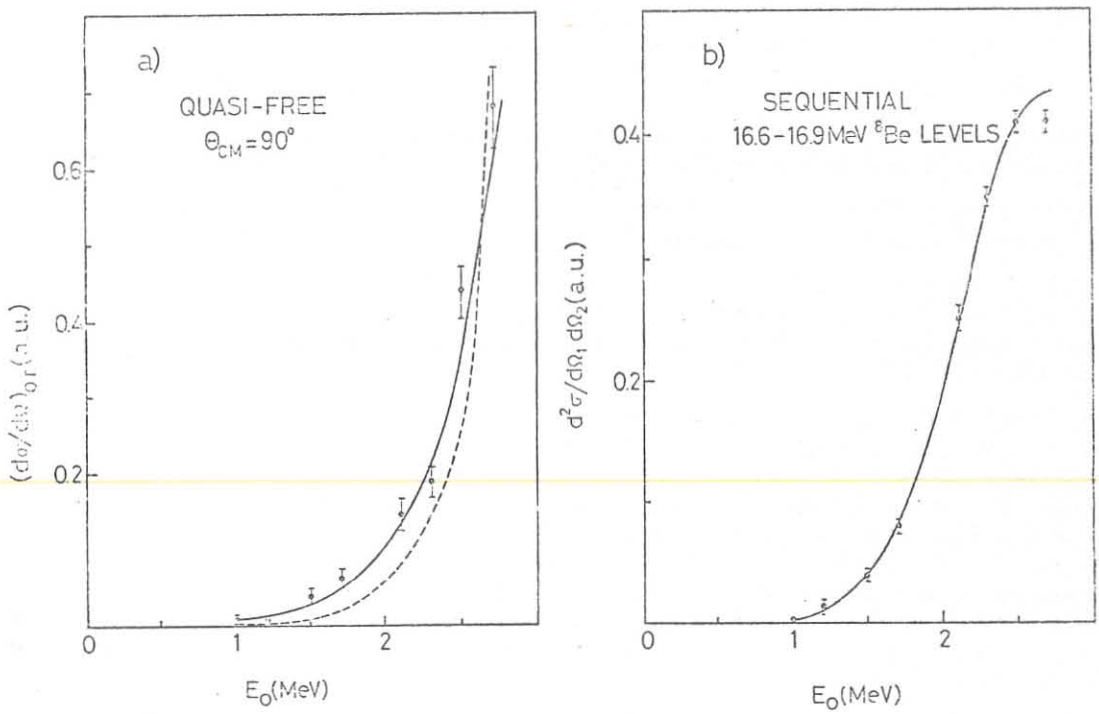

FIG. 5- Excitation functions of the sequential and QF processes. The fitting curves have been obtained through a parabolic approximation of the optical model potential. If the points at E_o = 2.5 MeV are divided by two, to compensate possible overstimation of the cross section, the dashed curve is obtained.

as a function of the laboratory incident energy.

Differential reaction cross section are usually calculated in the optical model framework. Here we are faced with a different kind of information, namely the excitation function, at given angle, of the sequential and QF processes. Hence we thought it useful to compare them with the behaviour of the total reaction cross section for ^{3}He on ^{9}Be as a function of the energy. In fact, effects due to the angular distribution should be excluded since the choice of the detection angles is such that θ_{CM} is always 90^o for the QFR at $p_S=0$ while it moves a few degrees around 88^o for the sequential peak.

If we assume that the probability to have a reaction is equal to the probability for the ^{3}He incident particle to cross the potential barrier, thus neglecting the contribution to the elastic channel, the total reaction cross section can simply be calculated in terms of the transmission coefficient T_l of the incident particle as

$$\sigma_R = \frac{\pi}{k^2} \sum_l (2l+1)\, T_l \qquad (6)$$

where $k=(2\mu E_o/\hbar^2)^{1/2}$, μ being the system reduced mass. In fact, this is equivalent to consider that the incident ^{3}He is always absorbed, after crossing the potential barrier region. In addition, a further approximation can be made since the transmission coefficients are sensitive only to the shape of the potential for energies comparable with the barrier itself. Within this assumption the real part of the potential can be approximated[6] by a parabola with the same top position and curvature. The transmission coefficient for a parabolic potential is given by

$$T_l = \left[1 + \exp\ (2\pi \frac{B_l - E_R}{\hbar \omega_l}) \right]^{-1} \qquad (7)$$

where B_l is the height of the barrier for angular momentum l, E_R is the C. M. incident energy and $\hbar \omega_l$ is given by:

$$\hbar\omega_l = \left[\frac{\hbar^2}{\mu} \left| \frac{d^2 V}{dr^2} \right| \right]^{1/2}$$

d^2V/dr^2 being the second derivative of the parabolic potential at the top; this last value can be calculated by taking the second derivative of the real part of nuclear potential at its maximum.

A Wood-Saxon real potential with V_o = 40 MeV, R=1. 17 $(A_1^{1/3} + A_2^{1/3})$ fm (A_1 and A_2 being the mass number of ^{9}Be and ^{3}He) and d=0. 65 fm gives B_o=1. 34 MeV and $\hbar \omega_o$ =2. 3 MeV.

A fit of the excitation function has been then performed both for the sequential and the QF processes using eqs. (6) and (7) and summing the contribution up to l_{max}=10. B_o and $\hbar \omega_o$ were considered as parameters, while the differences B_l-B_o were taken from the above calculation with the Wood-Saxon potential for r=7 fm, and $\hbar \omega_l = \hbar \omega_o$.

The results obtained show that the excitation function for the sequential process (5) can be well accounted for by eqs. (6) and taking B_o= (1.33 ± 0. 09) MeV and $\hbar \omega_o$ =(0. 81 ± 0. 08) MeV, with a χ^2 of 0. 35. Using these values of B_o and $\hbar \omega_o$ it is not possible to obtain a fit to the QF excitation function, since the χ^2 values range around 10^6. Instead a χ^2 = 3. 0 is obtained for B_o=2. 7 MeV and $\hbar \omega_o$=1. 58 MeV. A trial was also done, by dividing by two the experimental values of the cross section at energies lower than 2. 5 MeV. This procedure was intended to take into account possible overstimate of the QF cross section at low energies, due to the contribution of the sequential peaks (see for instance Fig. 1). Again a fit is obtained for B_o =2. 4 MeV, $\hbar \omega_o$=1. 07 MeV and χ^2=4. 8, which is reported as a dashed curve in Fig. 3. Even if the B_o value is reduced from 2. 7 to 2. 4 MeV, it is still considerably higher than the theoretical value, 1. 33 MeV.

5. - CONCLUSIONS

It seems then that, while the sequential process is clearly dominated by barrier penetration effects, the QF reaction shows influence of a different process. We have now to consider those perturbing effects which act differently in the sequential and QF processes. First, we may have a modulation of the cross section around resonances of the entrance channel ^{3}He+^{5}He. Actually a resonance is expected at $E_{^3He}$ = 1. 9 MeV, corresponding to an excitation energy of ^{8}Be of 22. 6 MeV. Unfortunately the measurement done right at this energy could not be used, due to a failure of the charge integrator. This resonance however, if present, should not affect the overall behaviour of the excitation function. Another process is of course a change in P due to absorption of the waves of the two outgoing α-particles, but P should not vary very much with the incident energy, since, by changing it from 1 to 2. 7 MeV, the α-particle energy is changed only from 11 to 11. 7 MeV (for E_S=0). Finally we evaluated possible rescattering effects following ref[7]. These effects are not expected to dominate the cross section, but we verified that the possible contributions due to formation of known ^{8}Be levels, in the 1-S or 2-S rescattering systems, do not fall in the energy region of interest in the α-particle spectra. Hence, the excitation function at θ_{CM}=90° for the ^{9}Be(^{3}He,$\alpha\alpha$)^{4}He QF reaction (Fig. 5b) is actually dominated by the energy dependence of the (off-shell) cross section of the ^{5}He(^{3}He, α)^{4}He virtual reaction (eq. (3)) which in turn cannot interpreted simply in terms of barrier effect.

In ref. [1] the angular distribution of reaction (3) at 4 MeV has been interpreted by a Butler approximation with cut-off radii R_c at 2. 9 and 5. 4 fm. With the latter value a zero is obtained in $j_l(k, R)$ for p_S=0 and $E_o \simeq$ 2. 4 MeV. Around this energy $(d\sigma/d\Omega)_{OT}$ would then have a minimum and the excitation function would raise at higher energies, with an apparent shift with respect to a simple barrier penetration effect. This effect can explain the high barrier effect we have found.

ACKNOWLEDGEMENTS

It is a pleasure to acknowledge the help of the technical staff of the V. d. G. accelerator, which ensured its smooth operation.

REFERENCES

1) - J. Kasagi, T. Nakagawa, N. Sekine, T. Tohei and H. Ueno, Nuclear Phys. 239A, 233 (1975).
2) - N. Arena, D. Vinciguerra, F. Riggi and C. Spitaleri, Lett. Nuovo Cimento 17, 231 (1976).
3) - P. G. Roos, N. S. Chant, A. A. Cowley, D. A. Goldberg, H. D. Holmgren and R. Woody, Phys. Rev. C15, 69 (1977).
4) - D. Miljianic, T. Zabel, R. B. Liebert, G. C. Phillips and V. Valkovic, Nuclear Phys. A215, 221 (1973).
5) - J. P. Génin, J. Julien, M. Rambaut, C. Samour, A. Palmeri and D. Vinciguerra, Lett. Nuovo Cimento 13, 693 (1975).
6) - D. L. Hill and J. A. Wheeler, Phys. Rev. 89, 1102 (1953).
7) - K. H. Bray, J. M. Cameron, G. C. Neilson and T. C. Sharma, Nuclear Phys. A181, 319 (1972).